Title

Solvent drag measurement of transcellular and basolateral membrane NaCl reflection coefficient in kidney proximal tubule.

Journal

The Journal of general physiology, 98(2)

ISSN

0022-1295

Authors

Shi, LB
Fushimi, K
Verkman, AS

Publication Date

1991-08-01

DOI

10.1085/jgp.98.2.379

Peer reviewed

Solvent Drag Measurement of Transcellular and Basolateral Membrane NaCl Reflection Coefficient in Kidney Proximal Tubule

LAN-BO SHI, KIYOHIDE FUSHIMI, and A. S. VERKMAN

From the Departments of Medicine and Physiology, Cardiovascular Research Institute, University of California, San Francisco, California 94143

ABSTRACT The NaCl reflection coefficient in proximal tubule has important implications for the mechanisms of near isosmotic volume reabsorption. A new fluorescence method was developed and applied to measure the transepithelial (σ^{TE}_{NaCl}) and basolateral membrane (σ^{bl}_{NaCl}) NaCl reflection coefficients in the isolated proximal straight tubule from rabbit kidney. For σ^{TE}_{NaCl} measurement, tubules were perfused with buffers containing 0 Cl, the Cl-sensitive fluorescent indicator 6-methoxy-*N*-[3-sulfopropyl] quinolinium and a Cl-insensitive indicator fluorescein sulfonate, and bathed in buffers of differing cryoscopic osmolalities containing NaCl. The transepithelial Cl gradient along the length of the tubule was measured in the steady state by a quantitative ratio imaging technique. A mathematical model based on the Kedem-Katchalsky equations was developed to calculate the axial profile of [Cl] from tubule geometry, lumen flow, water (P_f) and NaCl (P_{NaCl}) permeabilities, and σ^{TE}_{NaCl}. A fit of experimental results to the model gave $P_{NaCl} = (2.25 \pm 0.2) \times 10^{-5}$ cm/s and $\sigma^{TE}_{NaCl} = 0.98 \pm 0.03$ at 23°C. For measurement of σ^{bl}_{NaCl}, tubule cells were loaded with SPQ in the absence of Cl. NaCl solvent drag was measured from the time course of NaCl influx in response to rapid (<1 s) Cl addition to the bath solution. With bath-to-cell cryoscopic osmotic gradients of 0, −60, and +30 mosmol, initial Cl influx was 1.23, 1.10, and 1.25 mM/s; a fit to a mathematical model gave $\sigma^{bl}_{NaCl} = 0.97 \pm 0.04$. These results indicate absence of NaCl solvent drag in rabbit proximal tubule. The implications of these findings for water and NaCl movement in proximal tubule are evaluated.

INTRODUCTION

The mammalian proximal tubule is a leaky epithelium of one cell type that transports from lumen to capillary the majority of NaCl and water filtered by the kidney glomerulus. The reflection coefficient for NaCl across the paracellular pathway and the cell plasma membranes (transcellular pathway) is of fundamental importance for understanding the mechanisms of NaCl and volume reabsorption (Andreoli and

Address reprint requests to Dr. A. S. Verkman, Box 0532, Cardiovascular Research Institute, 1065 Health Sciences East Tower, University of California, San Francisco, CA 94143.

J. GEN. PHYSIOL. © The Rockefeller University Press · 0022-1295/91/08/0379/20 $2.00
Volume 98 August 1991 379–398

Schafer, 1978; Green and Giebisch, 1989), passive cell volume regulation (Welling and Welling, 1988), and the physical nature of the water transporting pathway (Finkelstein, 1987; Verkman, 1989). Because of the very rapid rates of NaCl and osmotic water transport in proximal tubule, accurate measurement of the NaCl reflection coefficient has been very difficult as evidenced by the widely different values reported from different laboratories using similar or independent experimental approaches.

In perfused kidney tubules from rat and rabbit, the transepithelial NaCl reflection coefficient (σ^{TE}_{NaCl}) has been measured from the volume flow induced by equal gradients of NaCl and an impermeant solute (Rector et al., 1966; Andreoli et al., 1979; Hierholzer et al., 1980) and by solvent drag (Jacobson et al., 1982; Corman and Di Stefano, 1983; Green and Giebisch, 1989). Values in the range of 0.35–1.0 have been reported. All measurements were made by timed collections of luminal fluid with fixed tubule length and using mean osmotic and solute gradients in the data analysis. In the basolateral membrane of the perfused rabbit proximal tubule, the measurement of rapid cell volume changes by a video technique gave a basolateral membrane NaCl reflection coefficient (σ^{bl}_{NaCl}) of 0.5 (Welling et al., 1987). In isolated apical and basolateral membrane vesicles from rabbit proximal tubule, NaCl reflection coefficients were ~ 1.0 as measured by independent induced osmotic and solvent drag techniques (Pearce and Verkman, 1989). From light scattering studies of osmotic water transport in rat apical membrane vesicles, σ^{ap}_{NaCl} was initially reported to be 0.5 (Pratz et al., 1986); however, later studies, which corrected for refractive index artifacts, concluded that σ^{ap}_{NaCl} was 1.0 (Van der Goot et al., 1989). Functional water channels are known to be present on the plasma membranes of intact proximal tubule cells and isolated membrane vesicles (Meyer and Verkman, 1987; Verkman, 1989).

Because of the physiological significance of σ_{NaCl} in proximal tubule and the active controversy over its value, we have used new and incisive experimental methodology and mathematical analyses to measure σ^{TE}_{NaCl} and σ^{bl}_{NaCl}. Experiments were performed in the isolated perfused proximal straight tubule (PST) from rabbit kidney. Measurements of σ^{TE}_{NaCl} and σ^{bl}_{NaCl} were made by solvent drag using the Cl-sensitive fluorescent indicator 6-methoxy-*N*-[3-sulfopropyl] quinolinium (SPQ; Illsley and Verkman, 1987). Steady-state gradients of Cl along the full length of a perfused tubule were measured by a quantitative imaging technique using SPQ as an indicator of luminal Cl concentration. Experimental results were compared with a mathematical model. The kinetics of Cl diffusion and solvent drag across the basolateral membrane were determined using SPQ as an intracellular indicator of Cl activity. Cl activity was measured continuously in response to imposed bath-to-cell Cl and osmotic gradients. The results and analyses indicate that NaCl solvent drag does not occur in rabbit proximal straight tubule.

METHODS

Tubule Perfusion

Kidneys from female New Zealand white rabbits (1.5–2 kg) were cut in coronal slices. Individual segments of PST (1.5–2 mm) were dissected in solution 1 (see Table I) at 4°C as described

previously (Burg et al., 1966; Fushimi et al., 1990). Tubules were transferred to a laminar flow bath (Strange and Spring, 1986) in which solutions were exchanged in under 0.5 s. Tubules were mounted at the perfusion site by a tightly fitting holding pipette of 40 μm inner diameter pulled from glass capillary tubes (Drummond Scientific Co., Broomall, PA) on a vertical pipette puller. An inner perfusion pipette was advanced concentrically 0.1 mm into the tubule. The collection site (distal end) was a loosely fitting holding pipette. The bath perfusion rate was 10 ml/min. Bath temperature was monitored by a microthermistor. The luminal perfusion rate was either > 100 nl/min using a gravity driven system or set to 3–100 nl/min using a nanoliter infusion pump (Harvard Apparatus Co., Inc., S. Natick, MA) driving a 10-μl syringe (Hamilton Industries, Two Rivers, WI). The syringe was connected to the perfusion pipette with polyethylene PE-10 tubing (Becton, Dickinson & Co., Parsippany, NJ.). Luminal perfusion rate was calibrated against set pump rate as described previously (Kuwahara and Verkman, 1988).

Image Analysis of Steady-State Cl Gradients

The luminal Cl concentration along the tubule length was determined by a ratio imaging technique. The tubule was perfused with solution 1 containing 2 mM SPQ (synthesized as

TABLE I

Solution Compositions

Solution	1	2	3	4	5	6	7	8	9	10
					mM					
Na	130	130	100	0	50	50	50	100	100	100
Choline	0	0	0	100	50	50	50	0	0	0
Cl	0	130	50	0	50	50	50	0	50	50
Isethionate	130	0	50	100	50	50	50	100	50	50
Raffinose	0	0	60	60	60	0	90	60	0	90
Osmolality	300	300	300	300	300	240	330	300	240	330

In addition, all solutions contained 5 mM glucose, 5 mM HEPES, 5 mM K isethionate, 5 mM Na phosphate (or choline phosphate when Na was 0), 1 mM Ca acetate, 1 mM Mg acetate titrated to pH 7.4 with NaOH. Solution osmolalities were checked on a freezing-point depression osmometer.

described by Krapf et al., 1988*a*) with or without 0.03 mM fluorescein sulfonate (FS, Molecular Probes, Inc., Junction City, OR). SPQ fluorescence is quenched by Cl, whereas FS fluorescence is Cl insensitive. Both probes are nearly impermeant and nontoxic to tubule function (Krapf et al., 1988*b*; Kuwahara et al., 1988).

Tubules were viewed with an inverted epifluorescence microscope (Nikon Inc., Melville, NY). The excitation source was a stabilized 100-W Hg arc lamp in series with a 10% transmission neutral density filter. For measurement of SPQ fluorescence, the filter set consisted of a 350 ± 5-nm six-cavity interference filter blocked to the infrared (Omega Optical Inc., Brattleboro, VT), a fused silica 400-nm dichroic mirror, and a low autofluorescence 420-nm cut-on filter. For measurement of FS fluorescence, a 450 ± 5-nm interference filter, 510-nm dichroic mirror, and 530-nm cut-on filter were used. There was no detectable SPQ fluorescence with the FS filter set or FS fluorescence with the SPQ filter set. For most experiments a ×10 objective (Nikon, Inc.; numerical aperture 0.25, working distance 3 mm) was used.

The image of the fluorescent tubule lumen was focused onto a silicon intensified target camera (SIT66, Dage-MTI, Inc., Michigan City, IN) operating at fixed gain. Eight-bit, 512 × 512 pixel images were digitized with a frame grabber (DT2861, Data Translation, Marlboro, MA) and auxiliary processing board (DT2858) in an 80286 computer with 80287 math

coprocessor. Camera gain and zero setting were adjusted so that pixel intensities were in the range 10–150 (maximum 256) to avoid nonlinearities as described previously (Dix and Verkman, 1990). Generally 50 individual images were averaged for each recorded image.

Image analysis routines were written in FORTRAN. The mean pixel intensity at position x from the perfusion site, $I(x)$, was calculated from an average of pixel intensities across the tubule using a horizontal measuring box which was slightly larger than the tubule. Camera background, $B(x)$, was determined at each x using a measuring box of identical size which was positioned well outside of the tubule. The autofluorescence background measured with the SPQ filter set, $F_{auto}(x)$, was determined by decreasing the luminal perfusion rate to 10 nl/min and replacing the bath solution with 150 mM KSCN to quench intracellular SPQ fluorescence. The autofluorescence background determined by this method was identical to that determined by replacing the luminal perfusate with SPQ-free buffer. $F_{auto}(x)$ was generally $< 10\%$ of $I_{SPQ}(x) - B_{SPQ}(x)$. There was no measurable autofluorescence background using the FS filter set. The concentration of chloride at position x, [Cl(x)], was determined by the Stern-Volmer relation,

$$[Cl(x)] = (R(x)^{-1} - 1)/K_{Cl} \quad (1)$$

where K_{Cl} is the Stern-Volmer constant for quenching of luminal SPQ by Cl (118 M^{-1}, Illsley and Verkman, 1987) and $R(x)$ is a corrected intensity ratio equal to the fraction of maximum SPQ fluorescence (at 0 Cl) that remained after quenching by Cl. $R(x)$ was calculated from a ratio of tubule images taken with SPQ and FS filter sets,

$$R(x) = \frac{[I_{SPQ}(x) - B_{SPQ}(x) - F_{auto}(x)]\,[I_{FS}(0) - B_{FS}(0)]}{[I_{FS}(x) - B_{FS}(x)]\,[I_{SPQ}(0) - B_{SPQ}(0) - F_{auto}(0)]} \quad (2)$$

$R(x)$ is unity at $x = 0$ (perfusion site) and decreases as [Cl] increases along the tubule. Note that $R(x)$ is independent of tubule geometry, indicator dilution, image focus, and shading effects. In some experiments, $R(x)$ was calculated from SPQ images recorded at a zero and nonzero bath Cl,

$$R(x) = [I_{SPQ}(x) - B_{SPQ}(x) - F_{auto}(x)]/[I_{SPQ}(x) - B_{SPQ}(x) - F_{auto}(x)]_{Cl=0} \quad (3)$$

In experiments where the tubule lumen was perfused with SPQ and FS, calculation of $R(x)$ by Eqs. 2 and 3 gave nearly identical results because the tubule position and lumen diameter were insensitive to changes in bath solution composition.

The dependence of SPQ and FS fluorescence on Cl concentration was calibrated using the physiological buffers (mixture of solutions 1 and 2) in the tubule perfusion pipette. Signal intensities were measured by the SIT camera and corrected for background. Increasing Cl did not alter FS fluorescence but quenched SPQ fluorescence with a Stern-Volmer constant of 115 ± 4 M^{-1}, similar to the value of 118 M^{-1} given above.

Measurement of Basolateral Membrane Cl flux

Tubule cells were loaded with SPQ at 37°C by a 10-min luminal perfusion with solution 8 in which 10 mM Na isethionate was replaced by 20 mM SPQ (Krapf et al., 1988*b*). Although SPQ permeability is very low, there is sufficient diffusion into cells under these conditions to give a measurable signal. The lumen solution was then switched to solution 8 to remove extracellular SPQ and bath temperature was lowered to 23°C. Fluorescence was excited and detected using the optical arrangement described above except that the intensifier/camera was replaced by a R928 photomultiplier (Hamamatsu Corp., Middlesex, NJ), and the ×10 objective was replaced by a ×16 quartz objective (numerical aperture 0.35, working distance 1.4 mm, E. Leitz, Rockleigh, NJ). To minimize background fluorescence, a rectangular measuring diaphragm was placed over a 0.25-mm segment of tubule. Data were filtered by a single pole electronic

filter with 0.3-s time constant and digitized by a 12-bit ADALAB analog-to-digital converter (Interactive Microware, State College, PA) in an 80286 computer. Data were acquired at a rate of 30 points/s and averaged over 1-s intervals.

Steady-State Model of Transepithelial Solvent/Solute Flux

The dissipation of transepithelial osmotic and NaCl gradients along the length of a perfused cylindrical tubule is calculated in the steady state in the absence of active salt transport.

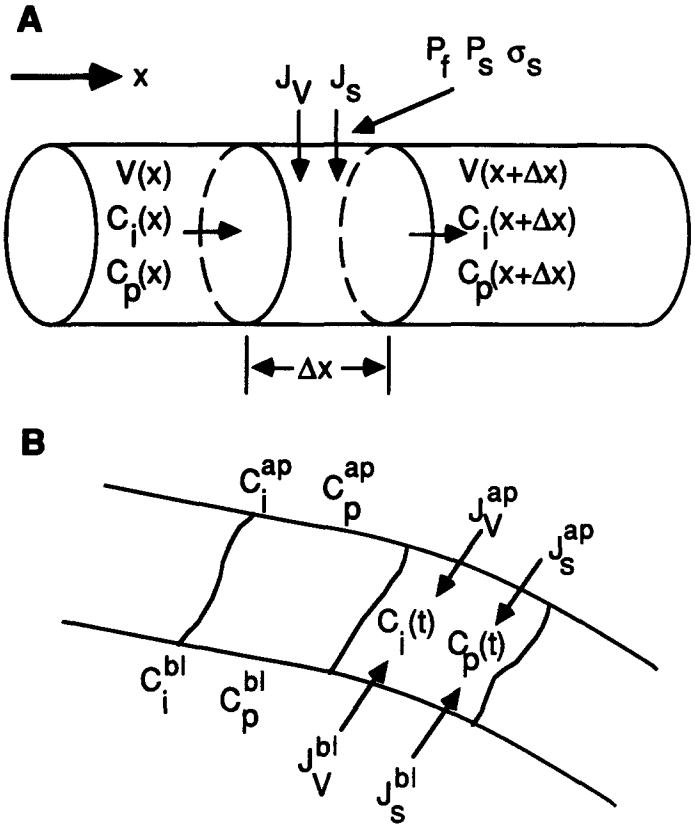

FIGURE 1. (*A*) Schematic diagram of a segment of perfused tubule showing bath-to-lumen transepithelial volume (J_V) and solute (J_s) fluxes. Luminal perfusion rate is $V(x)$. The transport characteristics of the whole epithelium are described by the parameters P_f, P_s, and σ_s (see text). (*B*) Schematic diagram of a proximal tubule cell showing apical and basolateral membrane volume and solute fluxes. Cell concentrations of impermeant and permeant solute are $C_i(t)$ and $C_p(t)$, respectively. See text for details.

Transepithelial transport is described by permeability coefficients for osmotic water (P_f) and solute (P_s) transport, and the solute reflection coefficient (σ_s). Fig. 1 *A* shows a segment of tubule with lumen flow $V(x)$, luminal impermeant solute concentration $C_i(x)$, and luminal permeant solute concentration $C_p(x)$. The transepithelial fluxes of volume and solute are $J_V(x)$ and $J_s(x)$, respectively, with bath-to-lumen flux defined as positive. At each point x, the

Kedem-Katchalsky equations (1958) relate J_V and J_s to P_f, P_s, σ_s, C_i, C_p, and the external (bath) concentrations of impermeant solute C_i^o and permeant solute C_p^o,

$$J_V = -P_f S v_w [(C_i^o - C_i) + \sigma_s(C_p^o - C_p)] \quad (4a)$$

$$J_s = P_s S(c_p^o - c_p) + (1 - \sigma_s) J_V \hat{C}_p \quad (4b)$$

where S is tubule surface area (cm^2/mm tubule length), v_w is the partial molar volume of water (18 cm^3/mol) and $\hat{C}_p$ is the mean concentration of permeant solute taken to be C_p^o when $J_V > 0$ and 0 when $J_V < 0$ in subsequent calculations. The first term in the J_s equation is diffusive solute transport and the second term is solvent drag.

In the steady state, the axial flow of the impermeant solute $C_i(x)V(x)$ is constant since no transepithelial movement of impermeant solute occurs,

$$C_i(x)V(x) = C_i(0)V(0) \quad (5)$$

Recognizing that $J_V = dV/dx$, and differentiating Eq. 5 to give $dV/dx = -[C_i(0)V(0)/C_i(x)^2]\, dC_i/dx$, Eq. 4*a* becomes,

$$dC_i(x)/dx = [C_i(x)^2/[C_i(0)V(0)]] P_f S v_w [[C_i^o - C_i(x)] + \sigma_s[C_p^o - C_p(x)]] \quad (6)$$

The concentration of permeant solute at $x + dx$ (Fig. 1 *A*) is equal to the sum of solute entering the disk by axial and transepithelial movement, divided by the volume entering the disk,

$$C_p(x + dx) = [C_p(x)V(x) + J_s dx]/[V(x) + J_V dx] \quad (7)$$

Recognizing that Eq. 7 is equivalent to $dC_p/dx = [J_s - C_p J_V]/V(x)$, and combining with Eqs. 4*a*, 4*b*, and 5,

$$\frac{dC_p(x)}{dx} = \frac{S\, C_i(x)}{C_i(0)V(0)} [P_s(C_p^o - C_p) - P_f v_w [(C_i^o - C_i) + \sigma_s(C_p^o - C_p)][(1 - \sigma_s)\hat{C}_p - C_p]] \quad (8)$$

Eqs. 6 and 8 describe the profiles of C_i and C_p along the tubule subject to initial conditions $C_i = C_i(0)$ and $C_p = C_p(0)$ at the perfusion site. The equations were integrated numerically by the forward Euler's method using 500 x-intervals. $R(x)$ was calculated from $C_p(x)$ (where C_p is 2NaCl) using Eq. 1.

Kinetic Model of Basolateral Membrane Solvent/Solute Flux

The time course of cell volume (V_c) and intracellular permeant concentration was calculated for a tubule cell as shown in Fig. 1 *B*. Apical and basolateral membrane P_f, P_s, and σ_s were specified independently as denoted by the superscripts ap (apical) and bl (basolateral). Luminal and bath concentrations of impermeant and permeant solute were specified in the limit of rapid luminal perfusion. The Kedem-Katchalsky equations relating J_V^{ap}, J_V^{bl}, J_s^{ap}, and J_s^{bl} to P_f^{ap}, P_f^{bl}, P_s^{ap}, P_s^{bl}, σ_s^{ap}, σ_s^{bl}, C_i^{ap}, C_i^{bl}, C_p^{ap}, C_p^{bl}, and the time-dependent intracellular concentrations, $C_i(t)$ and $C_p(t)$, consist of two sets of equations (as in Eqs. 4 *a* and 4 *b*) where appropriate superscripts are included. Recognizing that $dV_c/dt = J_v^{ap} + J_v^{bl}$, $d(C_p V_c)/dt = J_s^{ap} + J_s^{bl}$, and $C_i(t)V_c(t) = C_i(0)V_c(0)$,

$$dC_i(t)/dt = -C_i(t)^2(J_V^{ap} + J_V^{bl})/[V_c(0)C_i(0)] \quad (9a)$$

$$d[C_p(t)/C_i(t)]/dt = (J_s^{ap} + J_s^{bl})/[V_c(0)C_i(0)] \quad (9b)$$

Eqs. 9 *a* and 9 *b* were integrated with initial conditions $C_i = C_i(0)$ and $C_p = C_p(0)$. $C_p(t)$ was converted to the time course of fluorescence $F(t)$ by the Stern-Volmer relation, $F(t) = F_o/[1 +$

$K_{Cl}^{cell}C_p(t)/2]$, where K_{Cl}^{cell} was reported to be 18 M^{-1} (in concentration, rather than activity units) from an ionophore calibration procedure (Krapf et al., 1988*b*).

Fitting Procedure

A formal fitting procedure was used to estimate P_s and σ_s in experiments comparing the effects of osmotic gradients on steady-state axial Cl profiles (see Fig. 7) and time-dependent cell Cl influx via the basolateral membrane (see Fig. 8). In the determination of transepithelial NaCl reflection coefficient from axial profiles of Cl activity, P_s and σ_s were fitted by a two-parameter χ^2 minimization procedure. The minimization was carried out by fitting simultaneously the set of three curves (positive, negative, and zero cryoscopic osmotic gradients, 512 points in each curve) to the predictions of Eqs. 6 and 8 in which P_s and σ_s were varied. χ^2 was defined as the sum of the squared differences between measured and calculated $R(x)$; the sum was carried out over all 3 × 512 data points. The values of the fixed parameters (not being fitted) are given in the legend to Fig. 7. For determination of P_s and σ_s^{bl} in kinetic experiments, a similar two-parameter fitting procedure was used in which experimental data were compared with the predictions of Eqs. 9 *a* and 9 *b*. The values of the fixed parameters are given in the legend to Fig. 9.

RESULTS

Transepithelial NaCl Reflection Coefficient

Fig. 2 shows a series of fluorescence micrographs of an isolated PST from rabbit kidney that was perfused with the indicators SPQ and FS. The perfusion is from left to right. In the absence of Cl, there is little systematic variation in SPQ and FS fluorescence along the length of the tubule. When Cl was added to the bath solution, SPQ fluorescence decreased from left to right because of Cl accumulation in the perfusion solution. There was little systematic change in FS fluorescence. Upon addition of KSCN to the bath solution, the remaining tubule autofluorescence measured using the SPQ filter set was quite low. It is remarkable that there were numerous local variations in fluorescence intensity along the length of the tubule due to nonuniformities in tubule geometry, tubule position with respect to the image focal plane, illumination intensity, and camera gain (shading artifact). There was very little entry of SPQ into cells under the conditions of the experiment. In control studies in which luminal SPQ was present for 15 min and then washed out, the remaining fluorescence from intracellular SPQ was $< 1\%$ of that measured when SPQ was in the lumen.

Fig. 3 *A* shows that the local intensity variations affected SPQ and FS fluorescence in a parallel manner. Importantly, the fluorescence ratio profile $R(x)$ calculated from Eq. 2 was insensitive to the local optical factors and depended only on Cl concentration. A similar insensitivity to local variations was obtained using Eq. 3 in which $R(x)$ was calculated from SPQ ratio profiles measured in the presence and absence of bath Cl (Fig. 3 *B*). These results provide a ratiometric approach for measurement of steady-state profiles of Cl concentration along the length of a perfused tubule.

The profile $R(x)$ depends upon tubule geometry, lumen perfusion rate, luminal and bath solution compositions, the transepithelial permeabilities P_f and P_s, and the solute reflection coefficient σ_s (Eqs. 6 and 8). The effects of luminal perfusion rate and bath Cl concentration on $R(x)$ were examined. In Fig. 4 *A*, the tubule was

perfused with 0 Cl (solution 3, containing 2 mM SPQ) and bathed in solution 6 in which 50 mM isethionate was replaced by Cl. The decrease in $R(x)$ along the length of the tubule corresponded to increasing luminal [Cl]. With increasing luminal flow rate, there was less marked dissipation of the Cl gradient because of the decreased transit time through the tubule. The predictions of the mathematical model are given

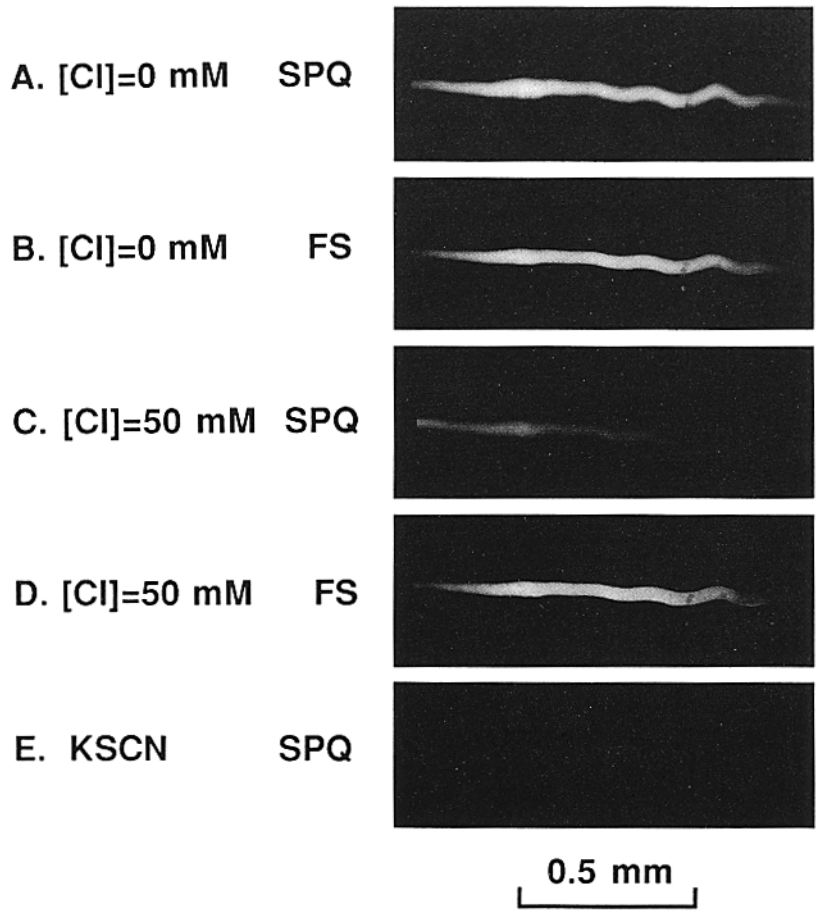

FIGURE 2. Fluorescence micrographs of proximal straight tubule perfused with SPQ and FS at 23°C as described in Methods. Images were recorded with the SPQ or FS filter sets as indicated. Lumen flow was 10 nl/min from left to right. Bath consisted of 0 Cl (solution 1), 50 mM Cl (mixture of solution 1 and 2), or 150 mM KSCN as indicated.

in Fig. 4 *B*. Model results were in close agreement with experiment for $P_s = 2 \times 10^{-5}$ cm/s. In four sets of similar experiments, P_s was $(2.0 \pm 0.3) \times 10^{-5}$ cm/s (SE). For these calculations, σ_s was taken to be unity (see below).

Fig. 5 *A* shows the dependence of $R(x)$ on bath Cl concentration for a constant 25 nl/min luminal perfusion rate. Increasing [Cl] resulted in lower fluorescence at any point along the tubule without a marked difference in the shape of the $R(x)$ profile.

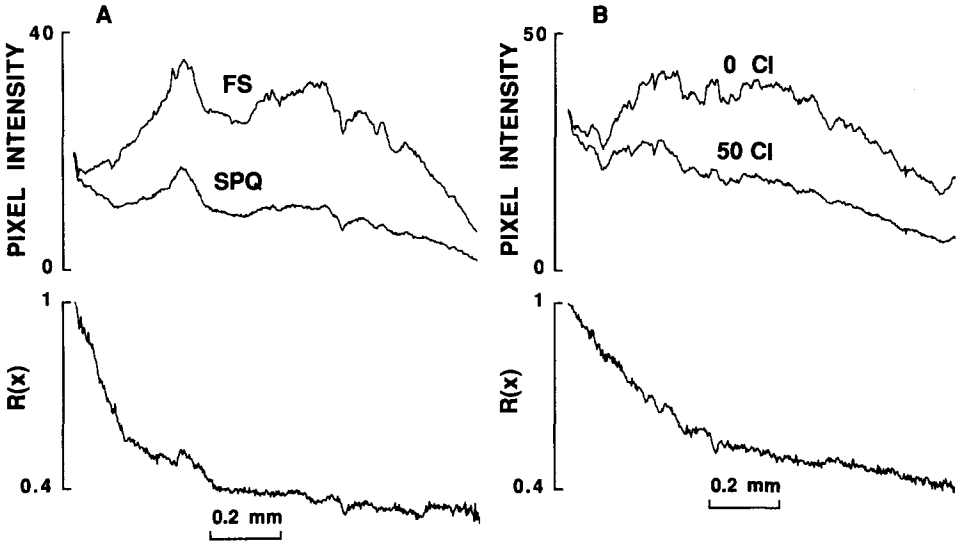

FIGURE 3. (*A*) Profiles of SPQ and FS fluorescence along the length of the tubule for 5 nl/min luminal perfusion and 50 mM bath Cl. Ordinate units are pixel intensities. The corrected intensity ratio $R(x)$ was calculated by Eq. 2. (*B*) Profiles of SPQ fluorescence at 0 and 50 mM bath Cl with 10 nl/min luminal perfusion. $R(x)$ was calculated from Eq. 3. Solutions 1 and 2 were used in this experiment.

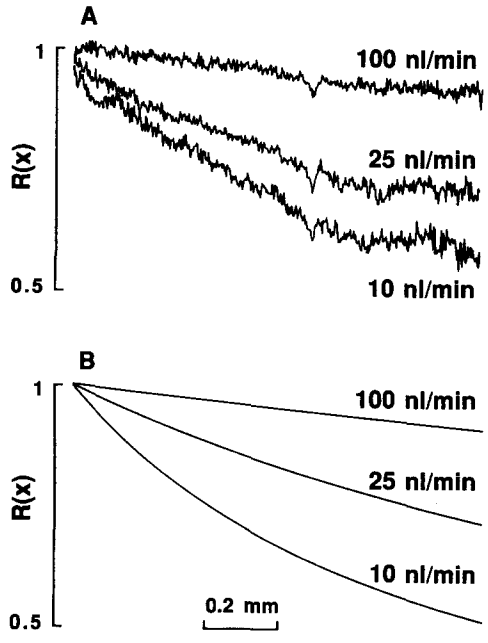

FIGURE 4. Dependence of the fluorescence intensity profile $R(x)$ on luminal perfusion rate. (*A*) Experimental data at 50 mM bath Cl (solution 3). The lumen was perfused with solution 8 at the indicated rates. (*B*) Model calculations (Eqs. 6 and 8) with P_s = 2×10^{-5} cm/s, P_f = 0.3 cm/s, σ_s = 1, S = 0.0013 cm^2/mm, C_i^o = 200 mM, C_p^o = 100 mM, $C_i(0)$ = 300 mM, $C_p(0)$ = 0 mM with $V(0)$ as indicated.

The bottom curve was obtained by decreasing the luminal perfusion rate to ~3 nl/min to equilibrate lumen and bath Cl at the distal end of the tubule. The fluorescence intensity remained constant beyond the position (0.1 mm) at which the Cl gradient was dissipated. The model results shown in Fig. 5 *B*, obtained using the same parameters as in Fig. 4 *B*, were in very good agreement with experiment. The difference between experiment and theory for the 3 nl/min perfusion study is probably due to the difficulty in maintaining accurate perfusion rates of under 10 nl/min.

The next set of studies were designed to determine whether solvent drag of NaCl from bath to lumen occurred. Tubules were perfused with 0 Cl and bathed in solutions of higher or lower cryoscopic osmolalities containing 25 or 50 mM Cl. The

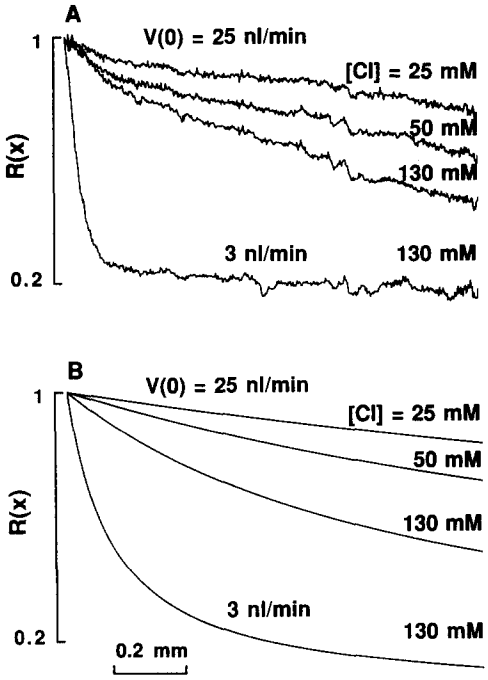

FIGURE 5. Dependence of fluorescence intensity profile $R(x)$ on bath Cl concentration. (*A*) Experimental data at 25 nl/min luminal perfusion rate (top three curves) and ~3 nl/min perfusion rate (bottom curve) with bath Cl concentrations indicated (mixture of solutions 1 and 2). (*B*) Model calculations with $P_s = 2 \times 10^{-5}$ cm/s, $P_f = 0.3$ cm/s, $\sigma_s = 1$, S = 0.0013 cm^2/mm, $V(0) = 25$ nl/min, $C_i^o = 40$–250 mM, $C_i(0) = 300$ mM, $C_p(0) = 0$ mM with $C_p^o = 50$–260 ([Cl] = 25–130 mM) as indicated.

mathematical model was used to optimize experimental design for best determination of σ_{NaCl}^{TE}. Fig. 6 shows a simulation in which external Cl was 50 mM, and a 60 mM cryoscopic osmotic gradient (bath lower than lumen osmolality) was imposed. As σ_s decreased (increasing NaCl solvent drag), the bath-to-lumen volume flux induced by the osmotic gradient enhanced the dissipation of the transepithelial Cl gradient. The effects were most marked at the proximal end of the tubule because of the high transepithelial volume flux. Experiments were also performed with bath > luminal cryoscopic osmolality because if σ_{NaCl}^{TE} were low, then bath-to-lumen volume flux and solvent drag would occur when bath and luminal cryoscopic osmolalities were equal (see below).

Fig. 7 *A* shows the measured $R(x)$ when bath solution contained 50 mM Cl and had cryoscopic osmolality equal to, 60 mosmol less than, and 30 mosmol more than luminal osmolality. The lumen perfusate contained no Na or Cl for application of Eqs. 6 and 8, in which it is assumed that Na and Cl move as a neutral pair.[1] The data, representing one set of experiments typical of six, showed little effect of osmotic gradient on the $R(x)$ profile. In all experiments, the curve labeled "−60 mosmol" was slightly above, and the curve labeled "+30 mosmol" was slightly below the "0 mosmol" curve. The results of a fitting procedure (see Methods) which gives best values for σ_{NaCl}^{TE} and P_s are shown as dashed curves. For the six sets of experiments, fitted parameters were (σ_{NaCl}^{TE}, P_s in units of 10^{-5} cm/s): (0.98, 2.32), (1.0, 2.05), (1.03, 2.50), (0.93, 1.99), (0.97, 2.40), and (0.97, 2.26). Averaged values were $\sigma_{NaCl}^{TE} = 0.98 \pm 0.03$ and $P_s = (2.25 \pm 0.2) \times 10^{-5}$ cm/s (SD).

The experiment was modeled in Fig. 7 *B* to give qualitative insight into the sensitivity of σ_{NaCl}^{TE} to curve shape. The curves were calculated for varying σ_{NaCl}^{TE}, comparing $R(x)$ in the absence of a cryoscopic osmotic gradient with that in the presence of a 60 mosmol lumen greater than bath gradient and a 30 mosmol bath greater than lumen gradient. For $\sigma_s = 1.0$, the −60 mosmol curve was highest

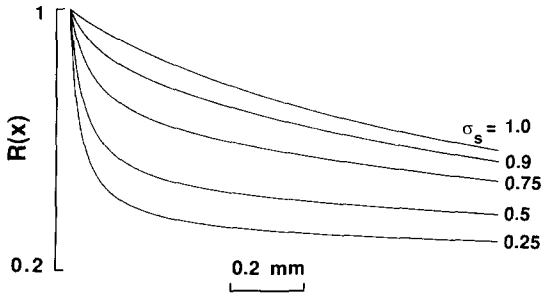

FIGURE 6. Theoretical dependence of $R(x)$ on σ_s for 50 mM bath Cl and a 60 mosmol lumen > bath osmotic gradient. Parameters: $P_s = 2 \times 10^{-5}$ cm/s, $P_f = 0.3$ cm/s, $S = 0.0013$ cm²/mm, $V(0) = 10$ nl/min, $C_i^o = 140$ mM, $C_p^o = 100$ mM, $C_i(0) = 300$ mM, $C_p(0) = 0$ mM with σ_s as indicated.

because bath-to-lumen volume flux caused dilution of lumen Cl. As σ_s decreased, the −60 mosmol curve became lowest because of solvent drag. The 0 mosmol curve became separated from the +30 mosmol curve. Model calculations showed that a σ_{NaCl}^{TE} of 0.9 would be easily distinguishable from unity.

Basolateral Membrane NaCl Reflection Coefficient

Tubule cells were loaded with SPQ for continuous measurement of intracellular Cl activity. Cl flux from bath to cell was induced by perfusing bath and lumen with 0 Cl and then rapidly replacing bath isethionate by 50 mM Cl in the presence or absence of an osmotic gradient between cell and bath. Solvent drag of NaCl from bath to cell in response to cell greater than bath osmolality would result in rapid influx of Cl at

[1] A set of similar experiments were performed on six tubules (three tubules at 50 mM bath Cl and three tubules at 25 mM Cl) in which the luminal perfusate was solution 8 (containing Na) instead of solution 4. Results were qualitatively and quantitatively similar to those obtained with solution 4, giving fitted values of $P_s = (2.1 \pm 0.2) \times 10^{-5}$ cm/s and $\sigma_{NaCl}^{TE} = 0.96 \pm 0.05$ (SD). It is recognized that the assumption that Na and Cl move as a neutral pair in Eq. 6 and 8 may not be valid when Na is present in the lumen.

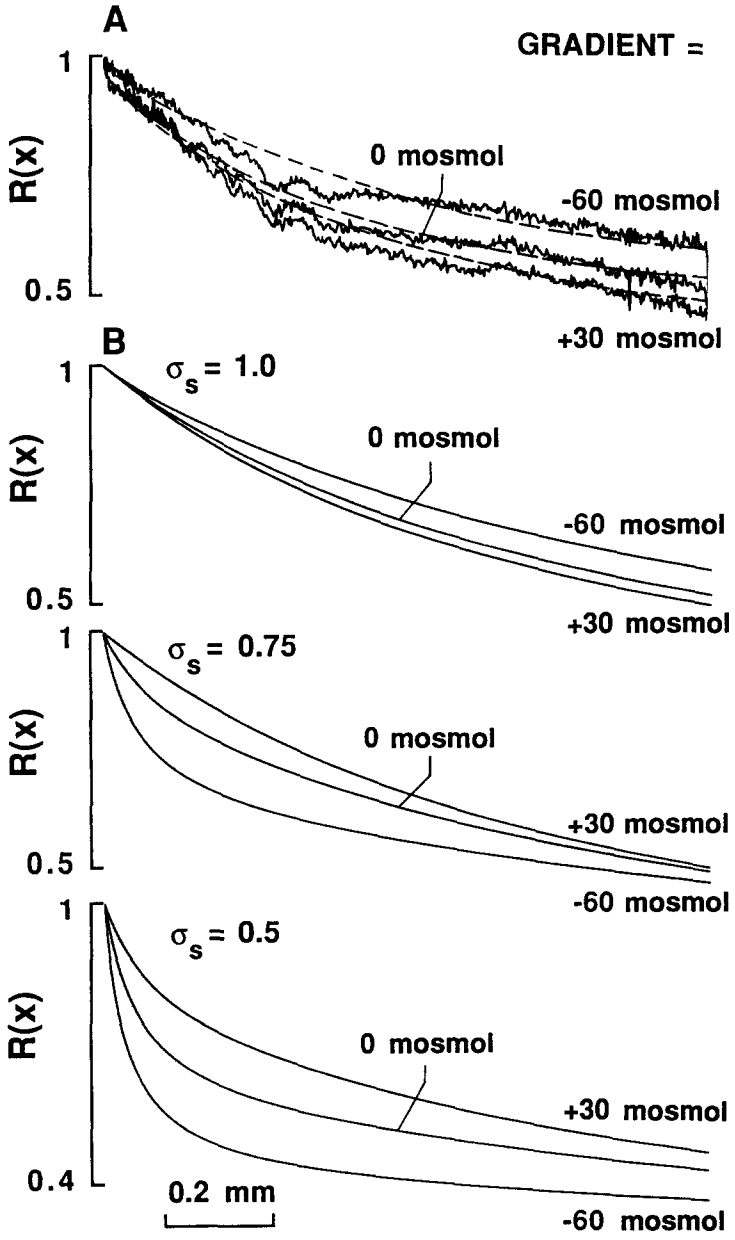

FIGURE 7. (*A*) Measurement of transepithelial NaCl solvent drag. Experimental data at 10 nl/min luminal perfusion rate (solution 4 in which 2 mM SPQ replaced 1 mM choline isethionate) and 50 mM bath Cl in the absence (solution 5) and presence of bath-to-lumen cryoscopic osmotic gradients of −60 mosmol (solution 6) and +30 mosmol (solution 7). $R(x)$ was calculated from Eq. 3 using solutions 2–5 as the 0 Cl reference solutions. The dashed curves through the data were calculated from a χ^2 minimization routine (see Methods) with fitted parameters $\sigma_s = 0.98$ and $P_s = 2.32 \times 10^{-5}$ cm/s. (*B*) Model calculations with $P_s = 2 \times 10^{-5}$ cm/s, $P_f = 0.3$ cm/s, $S = 0.0013$ cm^2/mm, $V(0) = 10$ nl/min, $C_i^o = 140$ mM (−60 mosmol) or 230 mM (+30 mosmol), $C_p^o = 100$ mM, $C_i(0) = 300$ mM, $C_p(0) = 0$ mM with σ_s as indicated.

early times after addition of Cl to the bath because of rapid water influx and cell swelling (Welling et al., 1987). Cl entry by passive diffusion is distinguishable from entry by solvent drag by its slower time course (see below).

Fig. 8 *A* shows the time course of intracellular SPQ fluorescence upon addition of Cl to and removal from the bath in the absence and presence of osmotic gradients.

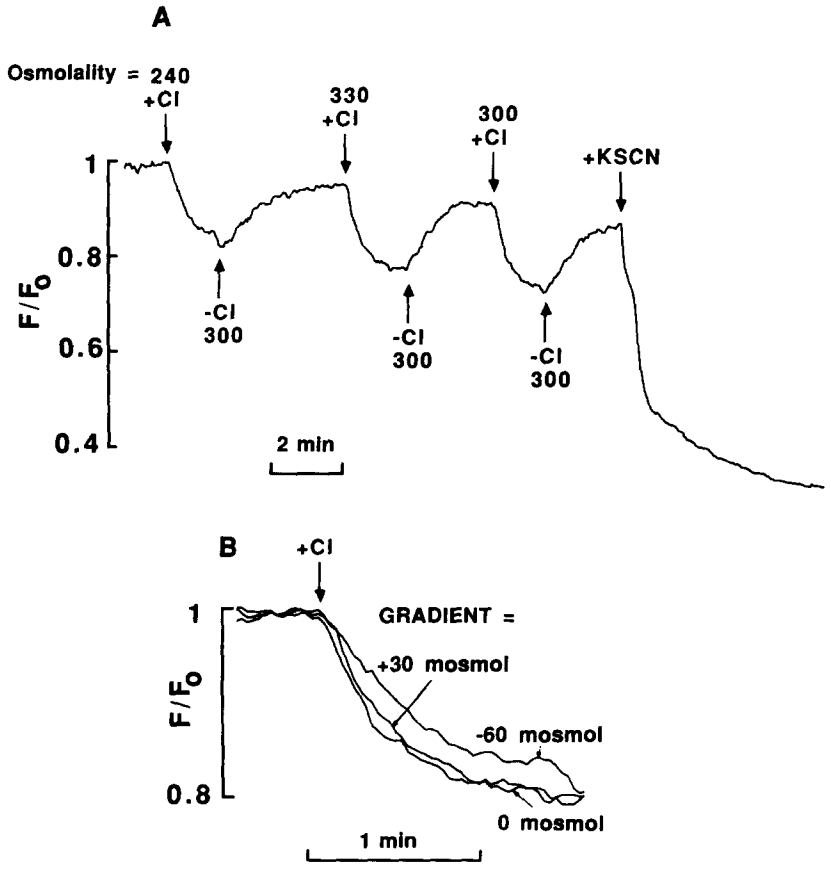

FIGURE 8. Measurement of basolateral membrane NaCl reflection coefficient. Tubule cells were loaded with SPQ and the time course of fluorescence was measured as described in Methods. The lumen was perfused with solution 8. The bath was perfused with solutions containing 0 mM Cl (300 mosmol, solution 8) or 50 mM Cl with different osmolalities (solutions 3, 9, and 10) as indicated. Bath solution was changed to 150 mM KSCN at the end of the experiment to give the baseline autofluorescence. Bottom curves are an expanded view of data immediately after each Cl addition.

KSCN was added at the end of the experiment to give the cell and instrumental background autofluorescence signal for calibration of absolute intracellular Cl activity (Krapf et al., 1988*b*). Expanded views of the phase of Cl entry (decrease in fluorescence) showed little effect of osmotic gradients (Fig. 8 *B*). In six sets of experiments, the initial rates of Cl entry were 1.23 ± 0.1 mM/s in the absence of a

cryoscopic osmotic gradient, 1.25 ± 0.1 mM/s in the presence of a 30 mM bath greater than cell osmotic gradient, and 1.10 ± 0.1 mM/s in the presence of a 60 mM cell greater than bath osmotic gradient. In separate control studies, 30 and 60 mM osmotic gradients did not alter SPQ fluorescence in the absence of Cl (not shown).

Fig. 9 shows the predictions of the kinetic model for Cl influx in the 3-compartment system (Eqs. 9*a* and 9*b*). σ_s values of 0.9 and below are distinguishable from unity. When σ_s is 1.0, the −60 mosmol curve is above the 0 mosmol curve because of intracellular dilution; as σ_s decreases, the −60 mosmol curve is below the other curves because of solvent drag. Fitting of experimental results from the six sets of experiments to the model described in Methods gave $\sigma_{NaCl}^{bl} = 0.97 \pm 0.04$ and $P_s^{bl} =$

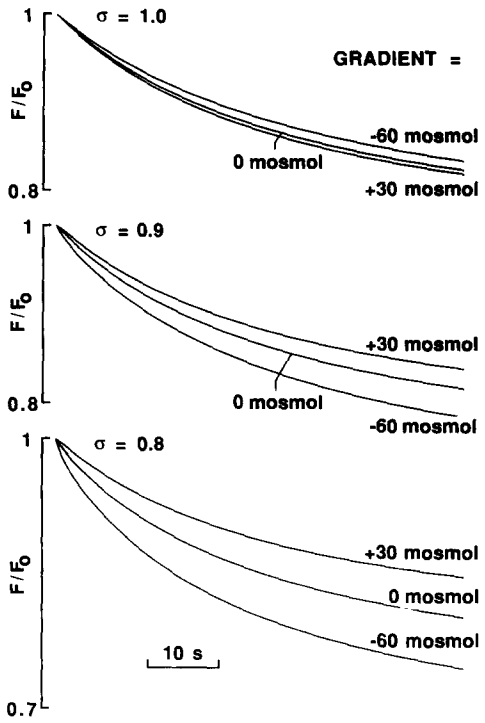

FIGURE 9. Mathematical model of basolateral membrane solvent drag. The experiments shown in Fig. 8 were modeled using Eqs. 9 *a* and 9 *b*. Parameters: $P_f^{ap} = 0.3$ cm/s, $P_f^{bl} = 0.2$ cm/s, $P_s^{ap} = 2 \times 10^{-5}$ cm/s, $P_s^{bl} = 3 \times 10^{-5}$ cm/s, $\sigma_s^{ap} = 1$, $C_i^{ap} = 300$ mM, $C_P^{ap} = 0$ mM, $C_P^{bl} = 100$ mM, $C_i(0) = 300$ mM, $C_P(0) = 0$ mM, $S = 0.0012$ cm²/mm, cell volume $= 3 \times 10^{-6}$ cm³/mm, with σ_s^{bl} as indicated and $C_i^{bl} = 200$ mM (0 mosmol gradient), 140 mM (−60 mosmol gradient), and 230 mM (+30 mosmol gradient).

$(2.8 \pm 0.4) \times 10^{-5}$ cm/s (SD). It is assumed in Eqs. 9*a* and 9*b* that Na and Cl move into the cell as a neutral pair. However, the analysis of initial slopes above, giving rates of Cl influx in units of millimolar per second, provides independent support for the conclusions that σ_{NaCl}^{bl} is near unity. The initial rate of Cl influx is the sum of fluxes due to diffusive transport and solvent drag. When the reflection coefficient is unity, the initial curve slopes are the same because volume flow does not influence initial Cl entry. As reflection coefficient decreases, the initial slope becomes strongly dependent upon osmotic gradient. For a reflection coefficient of 0.9, the ratio of initial slopes of the −60 mosmol curve to the +30 mosmol curve would be 1.38 for the parameter set used in Fig. 9. This difference in slope is not consistent with the

experimental results, indicating that the reflection coefficient must be significantly greater than 0.9.

DISCUSSION

The goal of these studies was to determine the transepithelial and basolateral membrane NaCl reflection coefficients in mammalian proximal tubule using an improved fluorescence methodology for measurement of solvent drag. NaCl solvent drag was detected by use of the Cl-sensitive fluorescent indicator SPQ. SPQ is nontoxic to cellular metabolism and is quenched by Cl by a collisional mechanism in a time much <1 ms (for review see Verkman, 1990). In apical and basolateral membrane vesicles from rabbit proximal tubule, SPQ was used to detect NaCl solvent drag (Pearce and Verkman, 1989). Vesicles containing SPQ and 0 Cl were mixed in 1 ms with hypo-osmotic solutions containing Cl. Because of the high sensitivity of SPQ fluorescence to Cl (50% quenching at 8 mM Cl), solvent drag-induced Cl influx could be measured during the phase of rapid osmotic water influx (<200 ms), before significant diffusive Cl entry occurred. It was found that σ_{NaCl} was not significantly different from unity in isolated membrane vesicles; differences in σ_{NaCl} of 0.02 were measurable. We have now extended this fluorescence methodology to measure solvent drag in the intact kidney tubule, where the interpretation of results is not confounded by the potential loss of a low reflection coefficient NaCl pathway in the vesicle isolation procedure or by the absence of intracellular components and regulatory/metabolic processes in vesicles.

The transepithelial NaCl reflection coefficient has been taken to be a phenomenological coefficient describing the movement of a neutral Na-Cl pair across a single barrier that in actuality consists of complex transcellular and paracellular pathways. It has been proposed that lumen-to-capillary volume flow can occur in the absence of a difference in cryoscopic osmolalities of luminal and capillary fluids if σ^{TE}_{NaCl} is much less than σ^{TE}_{NaHCO3} (Fromter et al., 1973; Green and Giebisch, 1984). However it is recognized that there are other quite plausible explanations for water reabsorption (Sackin and Boulpaep, 1975). Because the proximal tubule is highly water permeable, water transport may be driven by the relatively small degrees of luminal hypotonicity that have been measured (Liu et al., 1984; Schafer, 1984). Mechanisms of active solute transport resulting in lateral interspace hypertonicity have also been proposed (Diamond and Bossert, 1967).

Measurement of the transepithelial NaCl reflection coefficient was performed by a steady-state ratio imaging method. A time-resolved approach would not be suitable for theoretical and practical reasons. Pre–steady-state measurements of luminal Cl concentrations would be difficult to interpret because the proximal tubule consists of complex serial and parallel compartments. Also in practice, a lumen flow of ~ 5 nl/min must be maintained to prevent tubule collapse. The determination of Cl concentration along the full tubule length at different luminal perfusion rates and bath compositions provides greatly improved information content over the classical method of making a timed collection of luminal fluid at a single distance from the perfusion site, and single luminal perfusion rate and bath composition. A ratio imaging method was developed to determine absolute Cl concentration without

influence of tubule geometry, tubule position with respect to the focal plane, and local SPQ concentration.

There was no measurable solvent drag of NaCl in our experiments. Comparison of data with a phenomenological model for the accumulation of Cl along the length of a perfused tubule gave a best estimate of 1.0 for σ^{TE}_{NaCl}. The model assumed that Na and Cl moved as a neutral NaCl pair, and did not include complex ionic interactions and heteroporousity as evaluated by Weinstein (1987). The model did not include active salt transport because experiments were performed at 23°C in which >95% of active transport is inhibited. Osmotic water permeability was not measured in these studies; recent data from our laboratory obtained in rabbit proximal tubule under nearly identical conditions (Berry and Verkman, 1988) and similar results from other laboratories (for review, see Berry, 1983) were used in the calculations. Evaluation of the mathematical model for a wide range reported of P_f values (0.1–0.5 cm/s) did not change the best estimate of σ^{TE}_{NaCl} of 1.0.

The basolateral membrane reflection coefficient for NaCl has been reported to be ~0.5 from video measurements of cell volume in response to changes in bath osmolality (Welling et al., 1987). The interpretation of the video data was made difficult by the rapid and nonlinear changes in cell volume, finite bath exchange times and potential artifacts from solution refractive index. It was proposed that the presence of low and high reflection coefficient "pores" in the basolateral membrane might be important for passive volume regulation in proximal tubule (Welling and Welling, 1988). In basolateral membrane vesicles from rat and rabbit which contained functional water channels, σ^{bl}_{NaCl} was found to be unity (Pearce and Verkman, 1989; Van der Goot et al., 1989). It was argued that a low reflection coefficient pathway in the cell basolateral membrane would result in a large energetic burden to the cell (Pearce and Verkman, 1989). Capillary-to-cell solvent drag of NaCl through low reflection coefficient pores would deliver large quantities of Na that must be expelled by the Na/K ATPase. Furthermore, a low NaCl reflection coefficient pathway in the basolateral membrane must be matched by a similar pathway in the apical membrane to avoid rapid transcellular secretion of water.

The measurement of σ^{bl}_{NaCl} by solvent drag made use of intracellular SPQ as an indicator of the kinetics of capillary-to-cell Cl movement. SPQ was used previously to show that the steady-state intracellular Cl activity in rabbit proximal convoluted tubule was above electrochemical equilibrium (Krapf et al., 1988*b*). The data reported here indicate that osmotically driven water movement from capillary-to-cell did not result in measurable NaCl solvent drag. Comparison of data with a mathematical model gave a best value for σ^{bl}_{NaCl} of 1.0. The finding of a near unity NaCl reflection coefficient in basolateral membrane suggests that the water transporters are long narrow channels that exclude Na and/or Cl. This geometric interpretation is consistent with the near unity reflection coefficient for urea measured in basolateral membrane vesicles (Chen et al., 1988) and the high ratio of osmotic-to-diffusional water permeability in basolateral membrane of intact tubules (Verkman and Wong, 1987). The existence of a nonselective wide pore for water movement would be potentially deleterious to cell function if important small molecules could not be confined to the intracellular compartment.

The lack of NaCl solvent drag has implications for the mechanisms of transepithe-

lial water and salt movement. For a solute which traverses an epithelium by parallel transcellular (TC) and paracellular (PC) pathways, σ_s^{TE} is related to properties of the apical and basolateral cell membranes, and the paracellular pathway, by the relation,[2]

$$\sigma_s^{TE} = \frac{P_f^{PC}\sigma_s^{PC} + P_f^{TC}(\sigma_s^{ap}P_s^{bl} + \sigma_s^{bl}P_s^{ap})/(P_s^{ap} + P_s^{bl})}{P_f^{PC} + P_f^{TC}} \quad (10)$$

Eq. 10 shows that σ_s^{TE} can be low if the majority of water moves through a low reflection coefficient pathway. The reflection coefficient of the transcellular pathway is low when the rate-limiting membrane for solute transport has low reflection coefficient. It is notable that σ_s^{TE} can be low even if transcellular solute permeability greatly exceeds paracellular solute permeability, provided that the majority of water moves through the paracellular pathway and σ_s^{PC} is low.

The fraction of water which moves via the transcellular pathway is not known with certainty. It has been argued that the majority of water movement is transcellular (Berry, 1983) based on (*a*) high water permeability and functional water channels in the cell plasma membranes, (*b*) >80% inhibition of transepithelial water transport by mercurials (Berry and Verkman, 1988), and (*c*) measurements of paracellular solute permeability taken together with a pore model for paracellular water and solute movement (Preisig and Berry, 1985). However, an opposite conclusion was reported by Carpi-Medina and Whittembury (1988), in which >50% of transepithelial osmotic water flow was paracellular. If the water permeability of the transcellular pathway is much greater than that of the paracellular pathway, then the reflection coefficient for the rate-limiting plasma membrane for solute transport would be of greatest importance for determination of σ_s^{TE}.

Because Na and Cl do not move together across either membrane, it is not adequate to use a thermodynamic formalism to assign P_s^{ap} and P_s^{bl} values. Na moves via a Na/H antiporter and Na/glucose symporter on apical membrane, and Na/$3HCO_3$ symporter and 3Na/2K ATPase on basolateral membrane. Cl moves via a Cl/HCO_3 (formate) antiporter on apical membrane and probably Cl/Na-$2HCO_3$ antiporter on basolateral membrane. It is difficult to reconcile the thermodynamic formalism of solute-solvent coupling (Weinstein, 1983) with an explicit kinetic model of membrane transport (Verkman and Alpern, 1987).

Kedem and Leaf (1966) have evaluated the issue of separate reflection coefficients for individual ions of a cation–anion pair from a thermodynamic perspective. Two mathematical formulations were proposed. In the first, as used in the present work, the salt is considered to move as an electrically neutral pair. In the steady-state measurement of σ_{NaCl}^{TE}, this formulation would corresponding best to the experimental situation in which the lumen contained choline isethionate and the bath contained NaCl. In the kinetic measurement of σ_{NaCl}^{bl}, because intracellular K could not be removed without cell toxicity, it was necessary to assume that K and Cl do not move together through a low reflection coefficient pathway.

In the second formulation of Kedem and Leaf, the individual ions are considered

[2] Eq. 10 was derived from expressions for the reflection coefficients for serial barriers ($\sigma_s^{TC} = \sigma_s^{ap}\,P_s^{TC}/P_s^{ap} + \sigma_s^{bl}\,P_s^{TC}/P_s^{bl}$) and for parallel barriers ($\sigma_s^{TE} = [\sigma_s^{TC}\,P_f^{TC} + \sigma_s^{PC}\,P_f^{PC}]/[P_f^{TC} + P_f^{PC}]$) as given by Kedem and Katchalsky (1963).

to move independently through coupled or separate pathways. One important result was that if the anion and cation move through separate pathways, the apparent reflection coefficient will be that of the ion whose transport is rate-limiting. In the case of the intact proximal tubule, there are additional difficulties: (*a*) multiple pathways for Na and Cl transport exist, (*b*) the experiments were performed under highly non-equilibrium conditions, and (*c*) the transport of other ions (K, HCO_3) are coupled to Na and/or Cl. It is therefore very difficult to describe in a rigorous manner the complex electro-osmotic phenomena which operate when Na and Cl move through separate pathways.

Recognizing the inexact thermodynamic description of NaCl movement, our results show the absence of measurable NaCl solvent drag across the whole epithelium and basolateral plasma membrane in intact proximal straight tubule from rabbit. Results were obtained using new fluorescence methodology to image steady-state Cl gradients along the length of a perfused tubule and to detect solvent drag of NaCl from capillary to cell. Our data do not address whether NaCl solvent drag is present in other tubule segments and mammalian species.

This work was supported by grants DK-39354, DK-35124, and HL-42368 from the National Institutes of Health, a grant from the National Cystic Fibrosis Foundation, and a grant-in-aid from the American Heart Association. Dr. Fushimi is a fellow of the National Kidney Foundation. Dr. Verkman is an Established Investigator of the American Heart Association.

Original version received 10 April 1990 and accepted version received 11 February 1991.

REFERENCES

Andreoli, T. E., and J. A. Schafer. 1978. Volume absorption in the pars recta. III. Luminal hypotonicity as a driving force for isotonic volume absorption. *American Journal of Physiology.* 234:F349–F355.

Andreoli, T. E., J. A. Schafer, S. L. Troutman, and M. L. Watkins. 1979. Solvent drag component of Cl-flux in superficial proximal straight tubules: evidence for a paracellular component of isotonic fluid absorption. *American Journal of Physiology.* 237:F455–F462.

Berry, C. A. 1983. Water permeability and pathways in the proximal tubule. *American Journal of Physiology.* 245:F279–F294.

Berry, C. A., and A. S. Verkman. 1988. Osmotic gradient dependence of osmotic water permeability in rabbit proximal convoluted tubule. *Journal of Membrane Biology.* 105:33–43.

Burg, M., J. Grantham, M. Abramow, and J. Orloff. 1966. Preparation and study of fragments of single rabbit nephrons. *American Journal of Physiology.* 210:1293–1298.

Carpi-Medina, P., and G. Whittembury. 1988. Comparison of transcellular and transepithelial osmotic permeabilities in the isolated proximal straight tubule of rabbit kidney. *Pflügers Archiv.* 412:66–74.

Chen, P.-Y., D. Pearce, and A. S. Verkman. 1988. Membrane water and solute permeability determined quantitatively by self-quenching of an entrapped fluorophore. *Biochemistry.* 27:5713–5719.

Corman, B., and A. Di Stefano. 1983. Does water drag solutes through the kidney proximal tubule? *Pflügers Archiv.* 397:35–41.

Diamond, J. M., and W. H. Bossert. 1967. A mechanism for coupling of water and solute transport in epithelia. *Journal of General Physiology.* 50:2061–2083.

Dix, J. A., and A. S. Verkman. 1990. Mapping of fluorescence anisotropy in single cells by ratio imaging: application to cytoplasmic viscosity. *Biophysical Journal.* 57:231–240.

Finkelstein, A. 1987. Water Movement through Lipid Bilayers, Pores, and Plasma Membranes: Theory and Reality. 1st edition. John Wiley & Sons, Inc., New York. 66–80.

Fromter, E. E., G. Rumrich, and K. J. Ullrich. 1973. Phenomenological description of Na, Cl and HCO_3 absorption from proximal tubules in rat kidney. *Pflügers Archiv.* 343:189–220.

Fushimi, K., J. A. Dix, and A. S. Verkman. 1990. Cell membrane fluidity in the intact kidney proximal tubule measured by orientation-independent fluorescence anisotropy imaging. *Biophysical Journal.* 57:241–254.

Gonzalez, E., P. Carpi-Medina, and G. Whittembury. 1982. Cell osmotic water permeability of isolated rabbit proximal straight tubules. *American Journal of Physiology.* 242:F321–F330.

Green, R., and G. Giebisch. 1984. Luminal hypotonicity: a driving force for fluid absorption from the proximal tubule. *American Journal of Physiology.* 246:F167–F174.

Green, R., and G. Giebisch. 1989. Reflection coefficients and water permeability in rat proximal tubule. *American Journal of Physiology.* 257:F658–F668.

Hierholzer, K., S. Kawamura, D. W. Seldin, J. P. Kokko, and H. R. Jacobson. 1980. Reflection coefficients of various substrates across superficial and juxtamedullary proximal convoluted segments of rabbit nephrons. *Mineral and Electrolyte Metabolism.* 3:172–180.

Illsley, N. P., and A. S. Verkman. 1987. Membrane chloride transport measured using a chloride-sensitive fluorescent indicator. *Biochemistry.* 26:1215–1219.

Jacobson, H. R., J. P. Kokko, D. W. Seldin, and C. Holmberg. 1982. Lack of solvent drag of NaCl and $NaHCO_3$ in rabbit proximal tubules. *American Journal of Physiology.* 243:F342–F348.

Kedem, O., and A. Katchalsky. 1958. Thermodynamic analysis of the permeability of biological membranes to nonelectrolytes. *Biochimica et Biophysica Acta.* 27:229–246.

Kedem, O., and A. Katchalsky. 1963. Permeability of composite membranes. 3. Series array of elements. *Faraday Society Transactions.* 59:1941–1953.

Kedem, O., and A. Leaf. 1966. The relation between salt and ionic transport coefficients. *Journal of General Physiology.* 49:655–662.

Krapf, R., C. A. Berry, and A. S. Verkman. 1988*a*. Estimation of intracellular chloride activity in isolated perfused rabbit proximal tubules using a fluorescent probe. *Biophysical Journal.* 53:955–962.

Krapf, R., N. P. Illsley, H. C. Tseng, and A. S. Verkman. 1988*b*. Structure-activity relationships of chloride-sensitive fluorescent indicators for biological application. *Analytical Biochemistry.* 169:142–150.

Kuwahara, M., C. A. Berry, and A. S. Verkman. 1988. Measurement of osmotic water transport in perfused cortical collecting tubules by fluorescence microscopy. *Biophysical Journal.* 54:595–602.

Kuwahara, M., and A. S. Verkman. 1988. Direct fluorescence measurement of diffusional water permeability in the vasopressin-sensitive kidney collecting tubule. *Biophysical Journal.* 54:587–593.

Liu, F. Y., M. G. Cogan, and F. C. Rector. 1984. Axial heterogeneity in the rat proximal convoluted tubule. II. Osmolality and osmotic water permeability. *American Journal of Physiology.* 247:F822–F826.

Meyer, M. M., and A. S. Verkman. 1987. Evidence for water channels in proximal tubule cell membranes. *Journal of Membrane Biology.* 96:107–119.

Pearce, D., and A. S. Verkman. 1989. NaCl reflection coefficients in proximal tubule apical and basolateral membrane vesicles: measurement by induced osmosis and solvent drag. *Biophysical Journal.* 55:1251–1259.

Pratz, J., P. Ripoche, and B. Corman. 1986. Osmotic water permeability and solute reflection coefficients of rat kidney brush-border membrane vesicles. *Biochimica et Biophysica Acta.* 861:395–397.

Preisig, P. A., and C. A. Berry. 1985. Evidence for transcellular osmotic water flow in rat proximal tubules. *American Journal of Physiology.* 249:F124–F131.

Rector, F. C., M. Martinez-Maldonado, F. P. Brunner, and D. W. Seldin. 1966. Evidence for passive reabsorption of NaCl in proximal tubule of rat kidney. *Journal of Clinical Investigation.* 45:1060a. (Abstr.)

Sackin, H., and E. L. Boulpaep. 1975. Models for coupling of salt and water transport. *Journal of General Physiology.* 66:671–733.

Schafer, J. A. 1984. Mechanisms coupling the absorption of solute and water in the proximal nephron. *Kidney International.* 25:708–716.

Strange, K., and K. R. Spring. 1986. Methods for imaging renal tubule cells. *Kidney International.* 30:192–200.

Van der Goot, F., P. Ripoche, and B. Corman. 1989. Determination of solute reflection coefficients in kidney brush-border membrane vesicles by light scattering: influence of refractive index. *Biochimica et Biophysica Acta.* 979:272–274.

Verkman, A. S. 1989. Mechanisms and regulation of water permeability in renal epithelia. *American Journal of Physiology.* 257:C837–C850.

Verkman, A. S. 1990. Development and biological applications of chloride-sensitive fluorescent indicators. *American Journal of Physiology.* 259:C375–C388.

Verkman, A. S., and R. J. Alpern. 1987. Kinetic transport model for cellular regulation of pH and solute concentration in the renal proximal tubule. *Biophysical Journal.* 51:533–546.

Verkman, A. S., and K. W. Wong. 1987. Proton nuclear magnetic resonance measurement of diffusional water permeability in suspended renal proximal tubules. *Biophysical Journal.* 51:717–723.

Weinstein, A. M. 1983. Nonequilibrium thermodynamic model of the rat proximal tubule epithelium. *Biophysical Journal.* 44:153–170.

Weinstein, A. M. 1987. Convective paracellular solute flux: A source of ion-ion interaction in the epithelial transport equations. *Journal of General Physiology.* 89:501–518.

Welling, D. J., and L. W. Welling. 1988. Model of renal cell volume regulation without active transport: the role of the heteroporous membrane. *American Journal of Physiology.* 255:F529–F538.

Welling, L. W., D. J. Welling, and T. J. Ochs. 1987. Video measurement of basolateral NaCl reflection coefficient in proximal tubule. *American Journal of Physiology.* 253:F290–F298.